Available online at www.sciencedirect.com
ScienceDirect
Icarus 186 (2007) 204–217
ICARUS
www.elsevier.com/locate/icarus

Geologic mapping of the Amirani–Gish Bar region of Io: Implications for the global geologic mapping of Io

David A. Williams [a,*], Laszlo P. Keszthelyi [b], David A. Crown [c], Windy L. Jaeger [b], Paul M. Schenk [d]

[a] *School of Earth and Space Exploration, Arizona State University, Box 871404, Tempe, AZ 85287, USA*
[b] *Astrogeology Team, U.S. Geological Survey, 2255 North Gemini Drive, Flagstaff, AZ 86002, USA*
[c] *Planetary Science Institute, 1700 East Fort Lowell Road, Suite 106, Tucson, AZ 85719, USA*
[d] *Lunar and Planetary Institute, 3600 Bay Area Boulevard, Houston, TX 77058, USA*

Received 8 March 2006; revised 21 July 2006

Available online 27 October 2006

Abstract

We produced the first geologic map of the Amirani–Gish Bar region of Io, the last of four regional maps generated from *Galileo* mission data. The Amirani–Gish Bar region has five primary types of geologic materials: plains, mountains, patera floors, flows, and diffuse deposits. The flows and patera floors are thought to be compositionally similar, but are subdivided based on interpretations regarding their emplacement environments and mechanisms. Our mapping shows that volcanic activity in the Amirani–Gish Bar region is dominated by the Amirani Eruptive Center (AEC), now recognized to be part of an extensive, combined Amirani–Maui flow field. A mappable flow connects Amirani and Maui, suggesting that Maui is fed from Amirani, such that the post-*Voyager* designation "Maui Eruptive Center" should be revised. Amirani contains at least four hot spots detected by *Galileo*, and is the source of widespread bright (sulfur?) flows and active dark (silicate?) flows being emplaced in the Promethean style (slowly emplaced, compound flow fields). The floor of Gish Bar Patera has been partially resurfaced by dark lava flows, although other parts of its floor are bright and appeared unchanged during the *Galileo* mission. This suggests that the floor did not undergo complete resurfacing as a lava lake as proposed for other ionian paterae. There are several other hot spots in the region that are the sources of both active dark flows (confined within paterae), and SO_2- and S_2-rich diffuse deposits. Mapped diffuse deposits around fractures on mountains and in the plains appear to serve as the source for gas venting without the release of magma, an association previously unrecognized in this region. The six mountains mapped in this region exhibit various states of degradation. In addition to gaining insight into this region of Io, all four maps are studied to assess the best methodology to use to produce a new global geologic map of Io based on the newly released, combined *Galileo–Voyager* global mosaics. To convey the complexity of ionian surface geology, we find that a new global geologic map of Io should include a map sheet displaying the global abundances and types of surface features as well as a complementary GIS database as a means to catalog the record of surface changes observed since the *Voyager* flybys and during the *Galileo* mission.

Keywords: Jupiter, satellites; Io; Geological processes; Volcanism; Satellite, surfaces

1. Introduction

Io, the innermost of the four Galilean satellites of the planet Jupiter, is the most volcanically active body in the Solar System. The 4:2:1 Laplace resonance between Io, Europa, and Ganymede induces severe tidal heating within Io (Peale et al., 1979) that has produced >400 active and dormant volcanoes (Radebaugh et al., 2001; Schenk et al., 2001; Lopes et al., 2004). The intensity of Io's volcanism presents challenges to the geologic mapping of its surface. For example, no impact craters have been recognized in any *Voyager* or *Galileo* images at any resolution (McEwen et al., 1998a), attesting to a very young surface age (no more than a few tens of millions of years; McEwen et al., 2000a) and removing the impact cratering statistical tools for stratigraphic correlation of map units. Mountains and structural features are almost invisible in high-sun images of Io, and there are only a limited number of low-sun images that show these features. Nevertheless, despite these

* Corresponding author.
E-mail address: david.williams@asu.edu (D.A. Williams).

0019-1035/$ – see front matter
doi:10.1016/j.icarus.2006.08.023

challenges, it is desirable to map the surface of Io to identify: (1) the *types* of material units and structures present, which are valuable identifiers for the styles of geologic processes active on the surface; and (2) the *extents* to which these units and structures are found on Io, which indicate the relationships between these processes. The purpose of this paper is to discuss insights gained into the geologic materials units, structures and processes of Io through the mapping of the Amirani–Gish Bar region using *Galileo* images. This region of the antijovian hemisphere is typical of Io in regard to the range of visible surface features that can be mapped. Through an analysis of the mapping results from this region, a comparison to three previously mapped regions (Williams et al., 2002, 2004, 2005) using *Galileo* data, and a review of several *Voyager*-era maps, we discuss the implications for the global geologic map of Io that we are preparing using the new USGS combined *Galileo–Voyager* Io mosaics.

2. Background

Planetary mapping is a tool that enables the definition and characterization of surface features into process-related material units and structures and places them within their stratigraphic context, enabling recognition of the geologic evolution of an area, region, or planet, depending upon the scale of the mapping (e.g., Shoemaker and Hackman, 1962; Wilhelms, 1972, 1990; Tanaka et al., 1994). Because our mapping efforts are based on albedo variations, surface landform morphology, and/or color variations in *Galileo* spacecraft data (i.e., we have no in situ information on rock ages or lithologies), we use color, textural, and geomorphologic information to define geologic units. Based on comparison with results from terrestrial field mapping, only under ideal circumstances is remote sensing-based planetary mapping able to provide accurate three-dimensional characterizations of material units and their stratigraphic relationships. Nevertheless, Wilhelms (1990) points out that planetary geologic mapping remains a necessary and useful technique to aid in the interpretation of planetary surfaces until ground truth can be obtained, and helps to identify targets of importance for future investigations.

A series of global, regional, and local geologic maps of Io were produced from *Voyager* images obtained during the 1979 flybys (Schaber, 1980, 1982; Moore, 1987; Greeley et al., 1988; Schaber et al., 1989; Whitford-Stark et al., 1991; Crown et al., 1992). Although medium- to high-resolution (hundreds to tens of meters/pixel) coverage was largely limited to the subjovian hemisphere, these maps were used to identify a range of volcano morphologies (e.g., shield volcanoes, pit craters, calderas, cones) and eruption products (e.g., lava flows, pyroclastic blankets) on Io, to interpret the colors of volcanic features relative to possible magma compositions (e.g., Sagan, 1979; Young, 1984; Carr, 1986; Johnson et al., 1988), and to infer the sequence of volcanic eruptions in specific regions (e.g., Maasaw Patera; Moore, 1987). These maps showed that the surface of Io is dominated by complex, interfingered volcanic deposits from dozens of regionally active volcanoes, and that in specific regions it is possible to use planetary mapping to constrain the roles of various effusive vs explosive eruptions, the relative importance of (inferred) sulfurous vs silicate compositions, and the relationships between tectonic and volcanic processes. With the additional high-resolution coverage of the antijovian hemisphere and more accurate global color data obtained by multiple *Galileo* flybys of Io (e.g., McEwen et al., 1998b, 2000a, 2000b; Keszthelyi et al., 2001; Turtle et al., 2001, 2004), regional geologic mapping of some of the previously unmapped portions of the satellite has been possible (Williams et al., 2002, 2004, 2005).

Our ultimate goal is to use regional mapping to determine the most useful mapping techniques for generation of a post-*Galileo* global geologic map based on the newly released, combined *Galileo–Voyager* global mosaics of Io. To that end, we utilize experience gained from the production of four regional geologic maps. The map presented here is the last of the four; we chose an existing *Galileo* regional mosaic with the same

Table 1
Galileo mission encounters[a]

Mission	Flyby/orbit	Date
NOM	J0[b]	Dec. 7, 1995
NOM	G1	Jun. 29, 1996
NOM	G2	Sep. 6, 1996
NOM	C3	Nov. 6, 1996
NOM	E4	Dec. 18, 1996
NOM	E5[b]	Jan. 20, 1997
NOM	E6	Feb. 20, 1997
NOM	G7	Apr. 3, 1997
NOM	G8	May 7, 1997
NOM	C9	Jun. 27, 1997
NOM	C10	Sep. 18, 1997
NOM	E11	Nov. 7, 1997
GEM	E12	Dec. 16, 1997
GEM	E13[b]	Feb. 10, 1998
GEM	E14	Mar. 29, 1998
GEM	E15	May 31, 1998
GEM	E16[b]	Jul. 21, 1998
GEM	E17	Sep. 26, 1998
GEM	E18[b]	Nov. 22, 1998
GEM	E19	Feb. 1, 1999
GEM	C20	May 5, 1999
GEM	C21	Jun. 30, 1999
GEM	C22	Aug. 14, 1999
GEM	C23[b]	Sep. 16, 1999
GEM	I24	Oct. 11, 1999
GEM	I25	Nov. 26, 1999
GEM	E26	Jan. 4, 2000
GMM	I27	Feb. 22, 2000
GMM	G28	May 20, 2000
GMM	G29	Dec. 28, 2000
GMM	C30	May 25, 2001
GMM	I31	Aug. 6, 2001
GMM	I32	Oct. 16, 2001
GMM	I33[b]	Jan. 17, 2002
GMM	A34[b]	Nov. 5, 2002
GMM	J35[b,c]	Sep. 21, 2003

[a] NOM, Galileo Nominal Mission; GEM, Galileo Europa Mission; GMM, Galileo Millennium Mission. Orbit letter designates primary remote sensing target: J, Jupiter; I, Io; E, Europa; G, Ganymede; C, Callisto; A, Amalthea.
[b] No SSI data collected on these orbits.
[c] Galileo impact into Jupiter.

Table 2
Named volcanic features in the Amirani–Gish Bar region (refer to Fig. 1)

Name	Latitude (N)	Longitude (W)	Size (km)	Hot spot	Notes[b]	Origin of name
Euxine Mons	26.3	126.5	286.2	N		Io passed by here in her wanderings
Dusura Patera	37.5	119	68.6	Y	Detected by NIMS in multiple orbits	Nabataean sun god
Amirani Eruptive Center	24.5	114.7	431.5	Y	Detected by Voyager, Galileo SSI & NIMS, Keck	Georgian god of fire
Maui Eruptive Center	19.5	122.3	110.8	Y	Detected by Voyager, Galileo NIMS	Hawaiian demigod who sought fire from Mafuike
Maui Patera	16.6	124.2	37.8	Y	Detected by Galileo NIMS	Hawaiian demigod who sought fire from Mafuike
Shango Patera	32.3	100.5	90.2	N		Yoruba thunder god
Skythia Mons	26.2	99	253.4	N		Io passed by here in her wanderings
Monan Patera	19.7	105.4	112.9	Y	Detected by Galileo SSI & NIMS	Brazilian god who destroyed the world with fire and flood
Monan Mons[a]	15.2	104.5	297	N		Brazilian god who destroyed the world with fire and flood
Ah Peku Patera[a]	10.3	107	84	Y	Detected by Galileo SSI & NIMS	Mayan thunder god
Estan Patera[a]	21.6	87.7	95		Detected by Galileo NIMS	Hittite sun god
Gish Bar Mons[a]	18.6	87.7	110	N		Babylonian sun god
Gish Bar Patera	16.2	90.3	122.2	Y	Detected by Galileo SSI & NIMS, Keck	Babylonian sun god

[a] Name provisionally approved by the IAU.
[b] From Lopes et al. (2004).

low-phase color, and as close to the same spatial resolution, as the new global mosaics (4° phase, 1 km/px) as the mapping base. The Amirani–Gish Bar region was observed by the *Galileo* Solid State Imager (SSI) in July 1999 (Orbit C21; see Table 1 for *Galileo* orbit designations) as part of a low-phase angle (∼4°) color observation of the antijovian hemisphere at 1.4 km/px, and in October 1999 (Orbit I24) at 490–570 m/px, through the clear filter at a moderate phase angle (20°–22°) during the first close flyby. From these observations, a composite regional mosaic, using the color from C21 and the spatial resolution of the I24 observation, was produced covering the Amirani–Maui eruptive centers, Skythia Mons, Shango Patera, Monan Mons and Patera, and Gish Bar Montes and Patera (Table 2, Fig. 1). The I24 observation was obtained using an image compression mode of the SSI that was belatedly discovered to have been damaged by radiation. The individual image frames of observation I24AMSKGI01 were scrambled following a specific and recognizable pattern, which JPL engineers identified and then developed software to largely unscramble (Keszthelyi et al., 2001). Thus, the images were partially restored and a useable mosaic could be generated, though artifacts do remain. Fig. 1 shows the I24AMSKGI01 mosaic merged with the C21 color. Although the spatial resolution of this merged mosaic (∼500–600 m/px) is better than the new global mosaics (1 km/px), it serves as a useful tool to help calibrate our global mapping techniques. Supplemental observations of Amirani from February 2000 (Orbit I27; Fig. 2) and Gish Bar from October 2001 (Orbit I32; Fig. 3) were also studied to aid in the mapping, as well as the low-sun mosaic from the primary *Galileo* mission to help identify mountains and scarp boundaries.

3. Constraints on Io mapping

Before we discuss our mapping results it is important to review briefly the challenges in mapping Io due to the nature of the available *Voyager* and *Galileo* data, relative to that of other planetary mapping programs. First, unlike lunar or martian orbiters that acquire images from a nearly constant orbit with uniform lighting conditions and spatial resolutions, *Galileo* and *Voyager* images of Io have a wide range of phase angles, lighting conditions, and image resolutions. This lack of uniformity in Io imaging coverage (i.e., global >1 km/px imaging, limited >100 to <1 km/px imaging, and rare <100 m/px imaging) places limits on the level of detail that can be represented. Second, as noted by Geissler et al. (1999, 2004), the bulk of the surface changes on Io are due to volcanism centered around a few very active vents, such as Pele and Prometheus. The initial analysis of *Galileo* global images shows that large areas of the surface (∼83%) had no discernable changes between the *Voyager* and *Galileo* missions (Geissler et al., 2004). The recognition that changes in Io's surface activity are related to specific (localized) volcanic sources suggests a mapping approach centered on formations (sets of related geologic units focused on a specific source of activity {patera, fluctus, mountain}). Third, because Io has a rich color pallet produced by the complex interaction of sulfur-bearing materials with silicates in an intense radiation environment, it is important to utilize the color data in mapping Io. Color data is particularly useful for identifying and mapping the surficial materials that may cover the surface to various extents. Specific details on the compositional inferences of Io's colors have been published elsewhere (Spencer et al., 2000; Geissler et al., 2001;

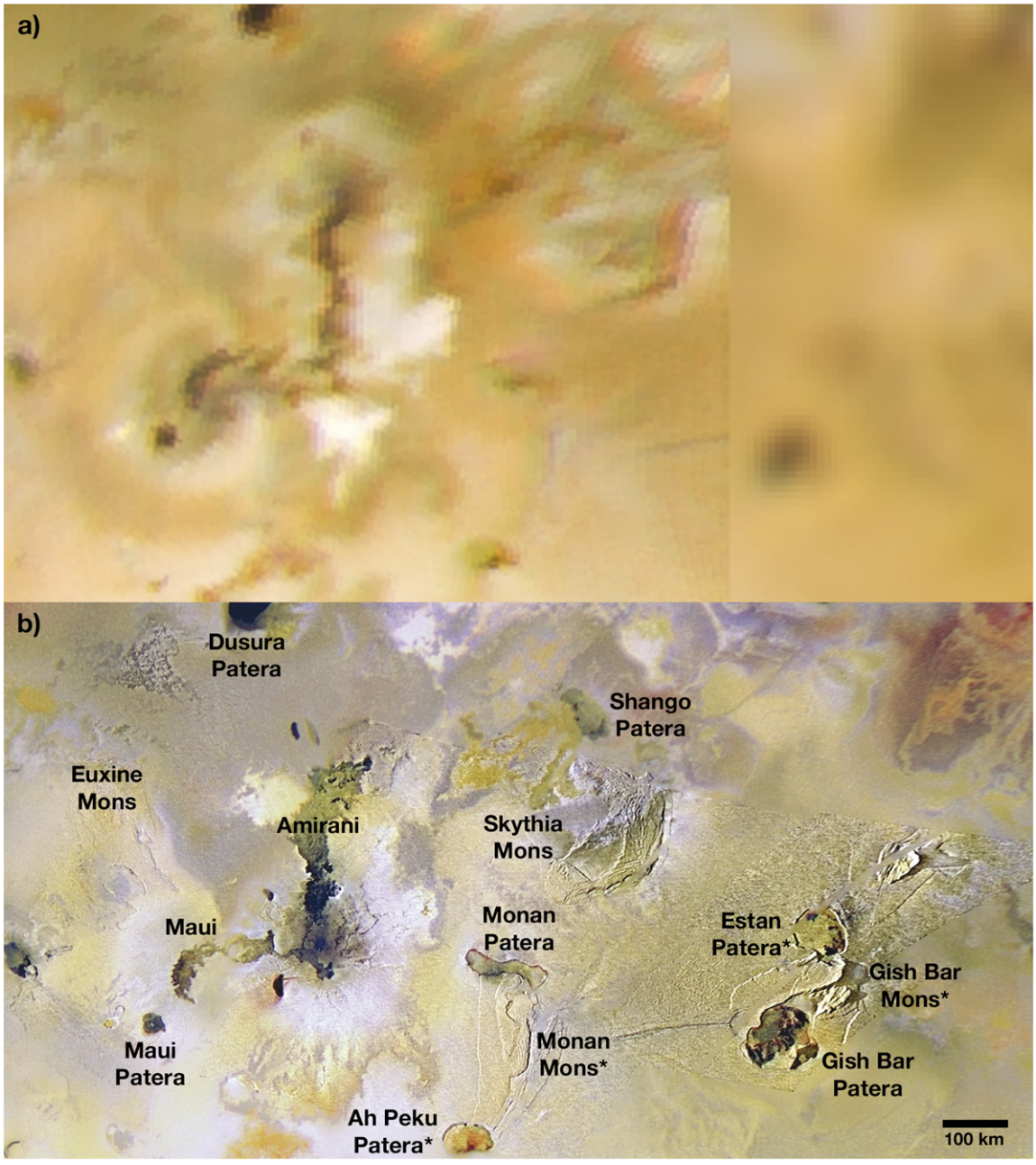

Fig. 1. (a) Best Voyager imaging of the Amirani–Gish Bar region (5–20 km/px). Extracted from global Voyager mosaic (NASA Photojournal PIA00319). (b) Galileo SSI mosaic covering the Amirani–Gish Bar region of Io. Mosaic is composed of reconstructed observation I24AMSKGI01 (490–570 m/px) merged with low-phase color observation C21COLOR01 (1.4 km/px). Feature names marked with an asterisk are provisionally approved by the IAU. The unusual texture in the I24 mosaic in the plains near Estan Patera and in other areas is an artifact of the image reconstruction process.

Williams et al., 2005), although important points for mapping are discussed later.

4. Map units and structures

Fig. 4 shows our geologic map of the Amirani–Gish Bar region, including a legend and correlation of map units. Fig. 5 shows color type localities for our map units. Important aspects of the geology and activity of the Amirani–Gish Bar region from direct *Galileo* SSI and Near Infrared Mapping Spectrometer (NIMS) image analysis have been discussed by McEwen et al. (1998a, 2000b), Lopes-Gautier et al. (1999), Keszthelyi et al. (2001), Douté et al. (2004), Lopes et al. (2001, 2004), Radebaugh et al. (2001), Schenk et al. (2001), and Turtle et al. (2001, 2004). Here we focus on new insights gained from the geologic mapping.

The major material units we selected for the Amirani–Gish Bar region are consistent with those chosen for previous regional geologic maps based on *Galileo* images (Williams et al., 2002, 2004, 2005), which in turn have a heritage going back to the *Voyager*-era maps (Moore, 1987; Greeley et al., 1988; Schaber et al., 1989; Whitford-Stark et al., 1991; Crown et al., 1992) and the units first defined by Schaber (1980, 1982). Es-

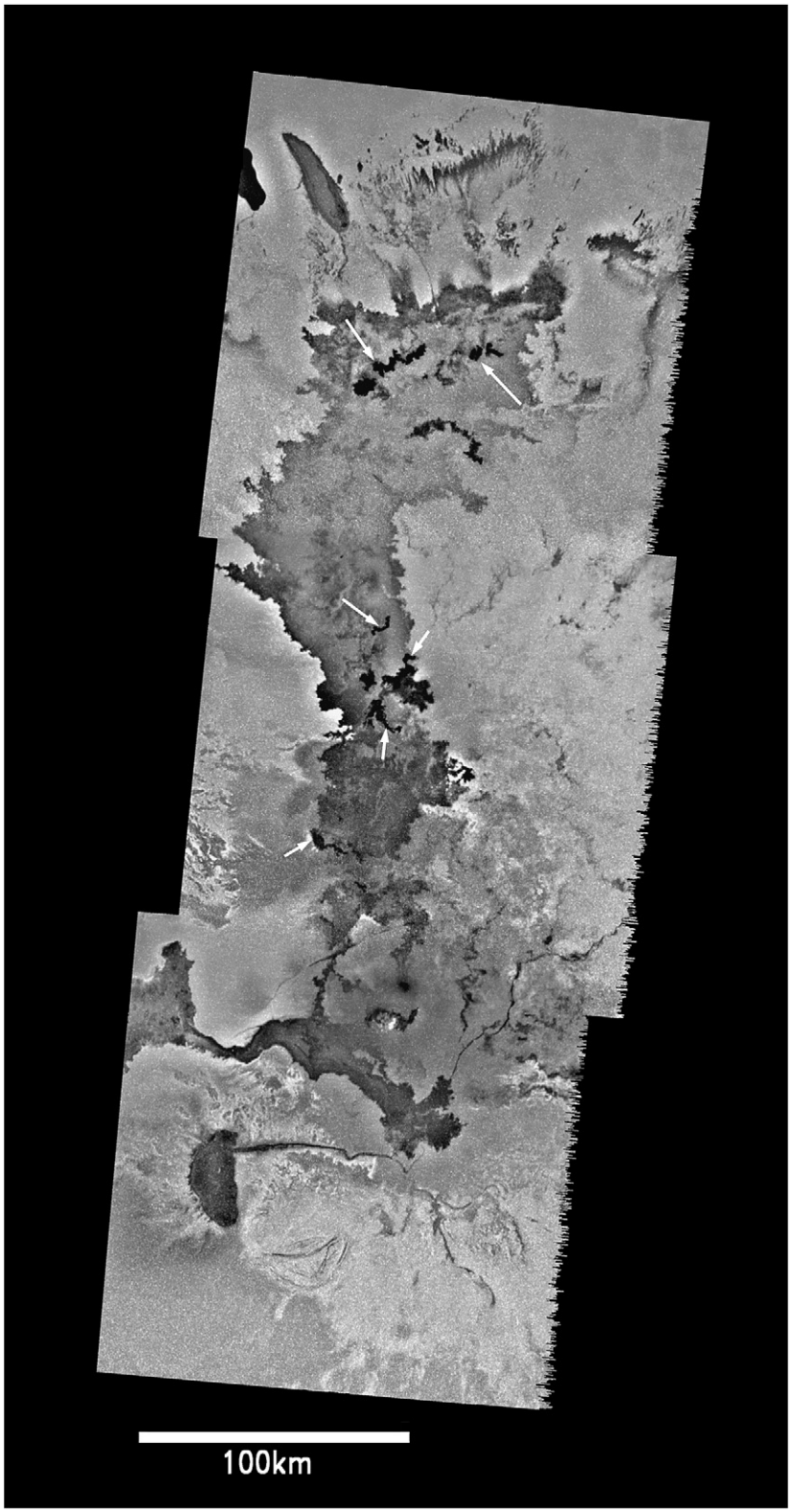

Fig. 2. Galileo SSI mosaic of the Amirani Eruptive Center (AEC), obtained during the Orbit I27 flyby (February 2000). Original resolution of the SSI images is 230–300 m/px. This is the highest resolution coverage of Amirani. Unlabeled white arrows indicate locations where changes in the dark flows are observed, based on comparison to I24 images (Keszthelyi et al., 2001).

sentially, Io has four general types of material units based on morphologic attributes first observed in *Voyager* images: mountain materials (i.e., tectonic massifs), flow materials (subdivided into patera floor materials, shield volcanoes, and a variety of flow fields), plains materials, and diffuse deposits. We now discuss in more detail aspects of the main geologic material units

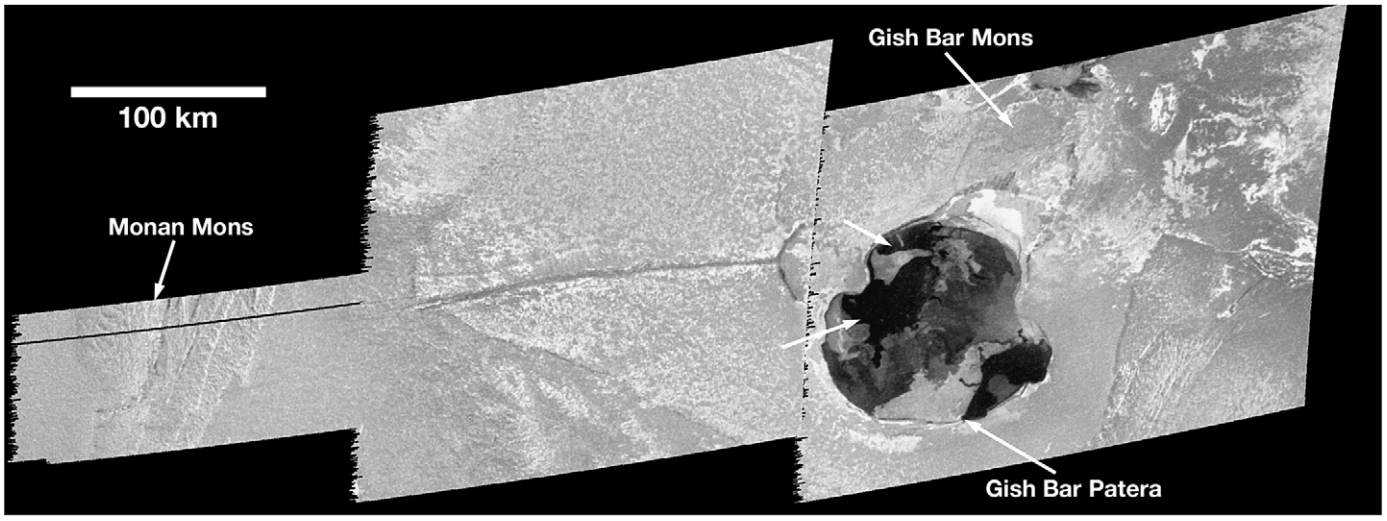

Fig. 3. Galileo SSI mosaic of central Monan Mons and Gish Bar Patera, obtained during the Orbit I32 flyby (October 2001). Original resolution of the SSI images is 340–350 m/px. This is the highest resolution coverage of Gish Bar Patera. Unlabeled white arrows show locations of changes in the patera floor, based on comparison to C21 and I24 images (modified from Turtle et al., 2004).

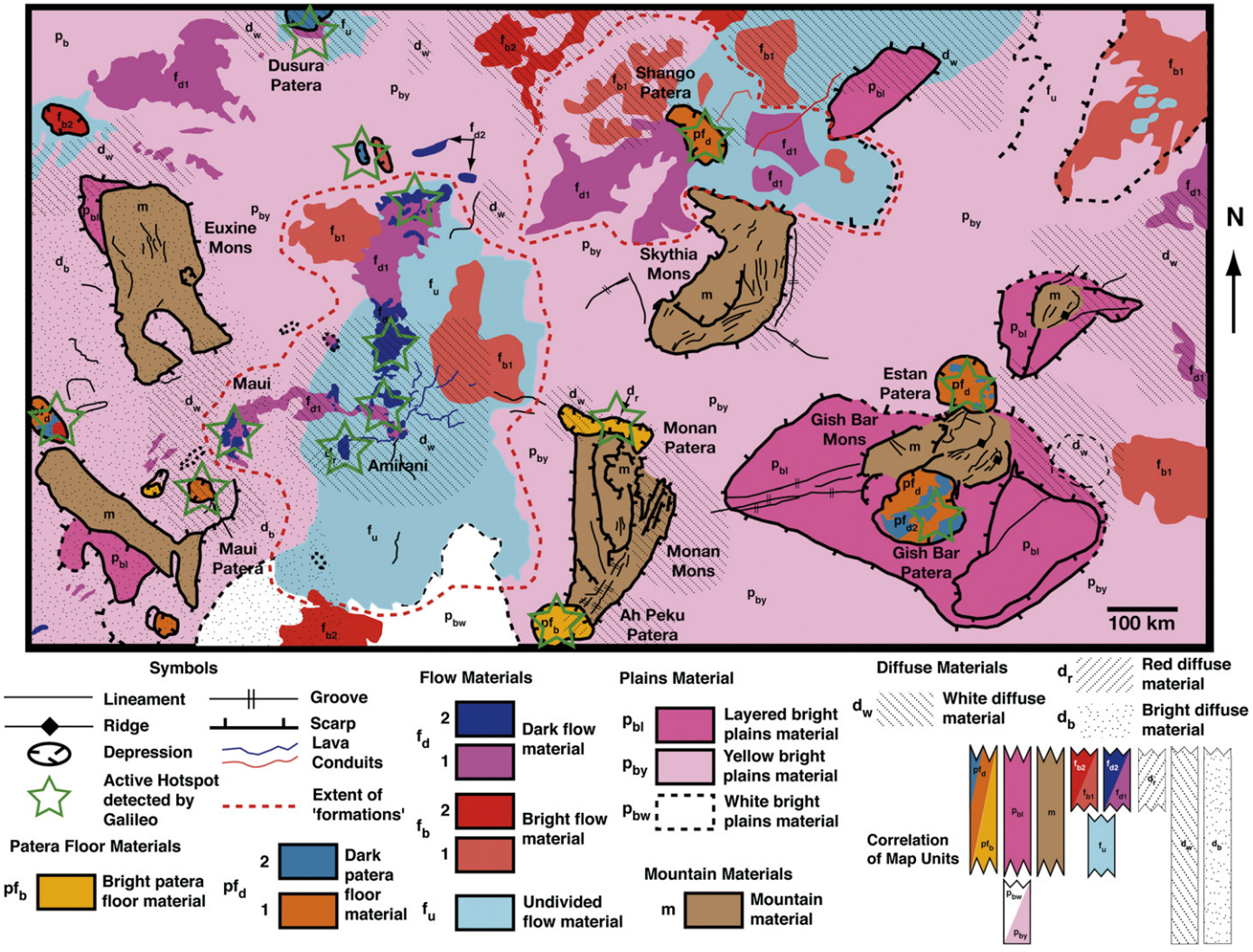

Fig. 4. Geologic map of the Amirani–Gish Bar region of Io, including legend and correlation of map units. Refer to Fig. 1b for image mosaic of the region, and Fig. 5 for map unit type localities.

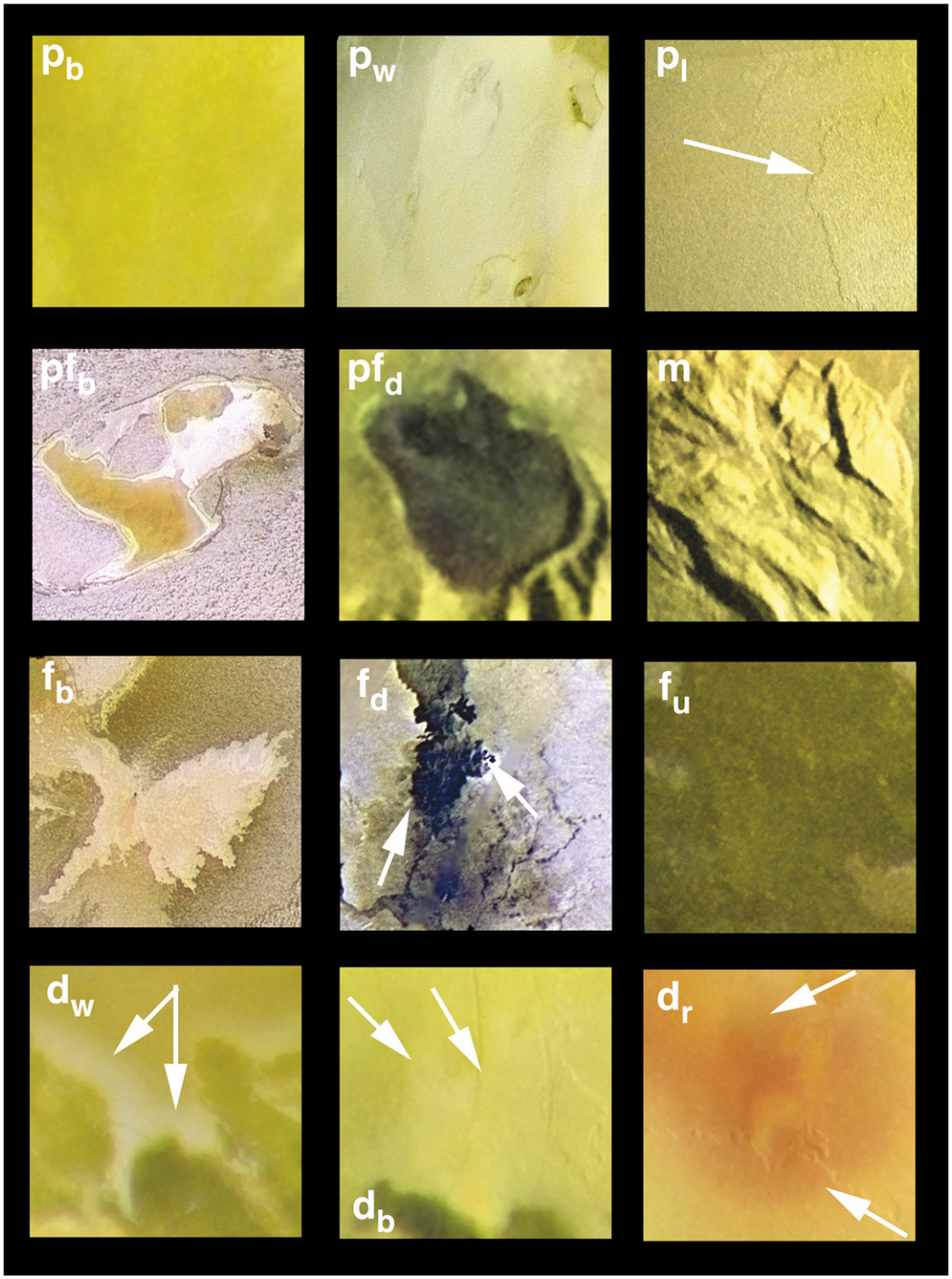

Fig. 5. Color type examples of material units found in the Amirani–Gish Bar region of Io. Bright plains materials (p_b), white plains materials (p_w), layered plains materials (p_l), bright patera floor materials (pf_b), dark patera floor materials (pf_d), mountain materials (m), bright flow materials (f_b), dark flow materials (f_d), undivided flow materials (f_u), white diffuse material (d_w), bright diffuse material (d_b), red diffuse material (d_r).

as they occur in the Amirani–Gish Bar region. Detailed descriptions and interpretations of these units are given in Table 3.

4.1. Plains materials

Plains materials cover more than 70% of Io's surface (Geissler et al., 1999), and appear in SSI color images as yellow, gray–white, and red to red–brown color units. The Amirani–Gish Bar region is dominated by Yellow Plains material, although a patch of White Plains material occurs south of the older Amirani bright flows adjacent to the distal ends of bright (presumably) sulfur flows from Emakong Patera (Williams et al., 2001) in Bosphorus Regio (off the southern end of the map). In general, the plains are interpreted as the

Table 3
Descriptions and interpretations of geologic material units found in the Amirani–Gish Bar region of Io, based on Galileo data analysis

Unit	R–G–B	Description	Interpretation
p_{by} Yellow Bright Plains Material	243–157–205 (pink)	Layered, textured surface, in various shades of yellow. Panchromatic albedo variation is considerable, but generally intermediate between Dark and Bright Patera Floor materials. Plains near volcanic centers are mantled by various types of diffuse materials or contain superposed lava flows. Plains contain scarps, grooves, pits, mesas, graben-like depressions, and/or channel-like features in some regions; scarp heights range typically from 50–100 m. At higher resolution, textured plains surface appears hummocky (i.e., periodic, km-scale mounds) and quite variable, from ill-defined on the stratigraphically lowest layers to prominently ridged on the stratigraphically highest layers (which tend to occur away from active volcanic centers). High-resolution images of the plains were not obtained in this region, but near Chaac Patera and Ot Mons individual hummocks were seen to be bright, irregular mounds in a matrix of darker, smoother material.	Silicate upper crust of Io mantled by (dominantly) sulfur-rich materials in brighter areas, with buried or partly buried silicate flows in darker areas. Surface deposits formed by a combination of volcanic plume fallout (i.e., diffuse deposits near specific vents such as Dusura and Shango) and frost deposition (i.e., frozen sulfurous gases from indeterminate sources that condense out of Io's variable atmosphere, covering wide areas). Processes that may form the hummocky texture include: (a) SO_2 sublimation, (b) dunes deposited by pyroclastic activity (McEwen et al., 2000b), (c) tectonic modification of crustal materials, (d) gravitational slumping (e.g., Moore et al., 2001), (e) tidal working of light surface materials (e.g., Bart et al., 2004). Orientations of the hummocks have been shown to be consistent with current tidal flexing (Bart et al., 2004).
p_{bw} White Bright Plains Material	255–255–255 (white, dashed border)	Layered, textured surface, white to white–gray in color. Panchromatic albedo variation is considerable, but generally intermediate between Dark and Bright Patera Floor materials. Hummocky texture and mantling may occur as described above.	Silicate upper crust of Io mantled by (dominantly) coarse- to intermediate-grained sulfur dioxide (SO_2) snow (see Douté et al., 2001) and perhaps other sulfur-bearing compounds that have been recrystallized from plume fallout.
p_{bl} Layered Bright Plains Material	245–67–151 (dk. pink)	Portions of Yellow and White Bright Plains materials as described above, that are isolated into plateaus and mesas by a scarp. The scarp may be lobate, digitate, unmodified, with alcoves, or with debris downslope (see Moore et al., 2001, for scarp classifications).	Silicate upper crust of Io, mantled by various materials, exposed on local topographic highs by a scarp resulting from degradational processes such as mass movement, SO_2 sapping, chemical decomposition, or some other processes (see Moore et al., 2001, for a good review).
pf_d Dark Patera Floor Material	0–100–150 (med. blue) (Subunit 2) 249–87–16 (dk. orange) (Subunit 1)	Dark gray to black surface with some variation in albedo and texture. Has distinct contact with surrounding terrain, and is found in topographic depressions that occur within paterae. In some regions at higher resolution (50 m/px) this material appears smooth and dark, and often correlates with NIMS and PPR hot spots; highest-resolution images of this material occur in the floor of Chaac Patera (Williams et al., 2002) and showed that this material can contain an interwoven mixture of relatively bright and dark features, irregular hummocks, and pits. Usually little sulfur dioxide is present, based on previous studies using NIMS data (Lopes et al., 2001). Subunit 2 is the darkest, freshest material.	Silicate lava flows that may or may not be coated by sulfurous materials (as indicated by brighter colors) or intermingled with various warmer silicate and sulfurous flows; black surfaces are likely warm, recently emplaced, coalesced silicate lava flows, or crusted lava lakes (Lopes et al., 2001; Davies et al., 2001; Radebaugh et al., 2004). Subunit 2 is equivalent to Flow materials subunit f_{d2}.
pf_b Bright Patera Floor Material	250–147–19 (lt. orange)	Bright pinkish-white to red-orange unit with smooth surface at high and medium resolution. Has distinct contact with surrounding terrain, usually found within paterae but can also occur on or beyond their rims. Galileo NIMS data indicate an enhanced signature of sulfur dioxide in the white to pinkish-white material on several paterae floors in other regions.	White, yellow and orange surfaces containing significant amounts of impure SO_2, requiring cold temperatures. Surfaces may be formed as coatings on cold silicate lava flows in less active paterae (e.g., Ah Peku Patera), as primary flows or 'ponds' of sulfur or SO_2, or as melting or sublimating Plains material being remobilized by heat from intrusions (e.g., paterae in the Chaac–Camaxtli region; Keszthelyi et al., 2004).
m Mountain Material	164–111–78 (lt. brown)	Yellow–gray to yellow–white unit that resembles Bright Plains, but that occurs on topographically elevated structures (e.g., mesas or plateaus, based on shadows) separated from plains by a bounding scarp. The bounding scarp is well-defined around most of these features. Unit contains grooves, ridges, scarps, and lineaments, some of which are suggestive of faulting or mass movement. Often these units are completely or partially covered with diffuse deposits.	An uplifted crustal block (mountain) that is undergoing erosion on all sides, possibly in the form of faulting or slumping.
f_d Dark Flow Material	20–28–137 (violet) (Subunit 2), 181–60–155 (purple) (Subunit 1)	At medium resolution, appears as smooth dark (black) lobate flows with lengths much greater than their widths. Contacts with surrounding terrain are sharp, and flows often extend toward and into apparent topographic lows (as indicated by mapping of scarps). Variation in albedos and cross-cutting relations can be used to define age relationships in some cases to separate younger (f_{d2}) from older (f_{d1}) flows. High-temperature hot spots usually correlate with dark flows as has been noted in NIMS and PPR observations (Lopes et al., 2001; Williams et al., 2002) both inside and outside paterae.	Lava flows of warm silicate materials from mafic or ultramafic silicate eruptions (see McEwen et al., 1998b; Williams et al., 2000). Range of albedos in dark flows due to variation in lava composition, coating of flow surfaces by sulfurous pyroclastic materials or condensates, or other effects of aging in the ionian environment.

(*continued on next page*)

Table 3 (*continued*)

Unit	R–G–B	Description	Interpretation
f_b Bright Flow Material	250–0–0 (red) (Subunit 2), 245–69–68 (red–orange) (Subunit 1)	At medium resolution, appears as smooth bright (yellow to white–gray) lobate flows with lengths greater than their widths. Contacts with surrounding terrain are sharp, and flows often extend toward and into apparent topographic lows (as indicated by mapping of scarps). Variation in albedos and cross-cutting relations can be used to define age relationships in some cases to separate younger (f_{b2}) from older (f_{b1}) flows. Rarely do NIMS hot spots correlate with bright flows (Williams et al., 2004) both inside and outside paterae.	Lava flows from sulfur or possibly sulfur dioxide eruptions (see Williams et al., 2001, 2002, 2004). Range of albedos in bright flows due to variation in lava composition, coating of flow surfaces by sulfurous pyroclastic materials or condensates, or other effects of aging in the ionian environment.
f_u Undivided Flow Material	100–197–219 (lt. blue)	Terrain consisting of bright and dark flows with a range of albedos. Contacts are not distinct, making it difficult to distinguish individual flow units.	Lava flows of indeterminate type, mostly likely from various Voyager-era or earlier silicate effusive eruptions, older than materials defined as f_d or f_b. Range of albedos due to coating of flow surfaces by pyroclastic materials or condensates, and/or the effects of aging in the ionian environment.
d_w White Diffuse Material	NW–SE diagonal hatching	White unit that appears to thinly mantle underlying materials, occurring mostly as circular patches around active vents or flows, or around grooves on mountains or in the plains. Generally shows decreasing optical depth with increasing distance from center of deposit.	Explosively emplaced pyroclastic deposits, probably dominated by sulfur dioxide. Volatiles may come from surficial deposits or near-surface 'aquifers' of SO_2 that are remobilized by nearby volcanic heat sources (as has been inferred to produce the radial white streaks around the Prometheus flow field; Kieffer et al., 2000; Milazzo et al., 2001), or from condensation of SO_2 gas from various plume eruptions.
d_b Bright Diffuse Material	Speckled hatching	Yellowish unit that appears to thinly mantle underlying materials, occurring mostly as circular patches around active vents, or as irregular patches streaming away from active vents. Generally shows decreasing optical depth with increasing distance from center of deposit. Generally individual deposits cover larger areal extents than White Diffuse Material.	Explosively emplaced pyroclastic deposits, probably colorized by sulfur-bearing particles. Volatiles most likely come from umbrella-like plumes from active volcanoes (e.g., Prometheus, Culann, Sobo Fluctus).
d_r Red Diffuse Material	NE–SW diagonal hatching	Dark red to red–brown unit that thinly mantles underlying materials, occurring primarily as an asymmetrical deposit W of a dark, unnamed, conduit-fed patera that is part of the Amirani Eruptive Center. This red unit has decreasing optical depth with increasing distance from the vent.	Explosively emplaced pyroclastic deposits rich in metastable, short-chain sulfur polymers (S_3 and S_4; Spencer et al., 1997) and/or sulfur-bearing chlorides (Schmitt and Rodriguez, 2003). The sulfur allotropes or chlorides could act as colorizing contaminants within bright, transparent material such as SO_2 (Geissler et al., 1999). Source appears to be primary magmatic S_2 or Cl_2 gas (Spencer et al., 2000; Keszthelyi et al., 2001; Schmitt and Rodriguez, 2003) coming from the vent.

Note. See Fig. 5 for type localities in color. R–G–B color values in column 2 represent R–G–B values used in Adobe Illustrator to produce colors of map units in Fig. 4. Modified from Williams et al. (2002, 2004, 2005).

silicate upper crust of Io with a mantle of sulfur-rich material, locally up to a few kilometers thick (Bart et al., 2004; Keszthelyi et al., 2004). Layered Plains materials occur as plateaus in both Yellow and White Plains materials, which have been observed in low-sun *Voyager* and *Galileo* images. These plateaus often have lobate, digitate margins and are thought to represent degradation of the plains by mass movement, SO_2 sapping, and/or chemical decomposition of sulfur-rich surface materials (Moore et al., 2001; Schenk et al., 2001). Compositionally, Yellow Plains are thought to be colored by substantial amounts of cyclo-octal sulfur (Geissler et al., 1999) or polysulfur oxides (Hapke, 1989), whereas the White Plains are thought to be purer, recrystallized sulfur dioxide snow (Carlson et al., 1997).

4.2. Lava Flow materials

We have characterized Lava Flow material units in the Amirani–Gish Bar region by their morphology, albedo and color, and recognize three types: Bright Flows (f_b), Dark Flows (f_d), and Undivided Flows (f_u). The characterization of Flow materials as Bright or Dark is inferred to have a compositional connotation (sulfur-dominated vs silicate-dominated, respectively). Correlation between NIMS and SSI data also shows that the darkest Flow materials appear to be associated with active hot spots (Lopes et al., 2001, 2004). Flows with intermediate albedos and colors (i.e., their original albedo and color cannot be determined) and/or ill-defined contacts with other units are classified as Undivided Flow materials. Two subunits, labeled 1 and 2, were used for both bright and dark flows based on their inferred relative ages; the youngest bright flows are very bright (high albedo, f_{b2}), the youngest dark flows are very dark (low albedo, f_{d2}). In SSI images, Flow materials are typified by their sharp contacts with the other units and generally elongated morphology (lengths $\gg$ widths; Williams et al., 2002, 2004, 2005). The limited high- and moderate-resolution images show irrefutable evidence at a number of sites that these units formed via viscous flows of lava (McEwen et al., 1998a, 2000b; Keszthelyi et al., 2001; Turtle et al., 2004). No positive relief volcanic constructs (small shields, cones, or domes) are observed in this region.

4.3. Patera Floor materials

Patera Floor units have a range of albedos and colors that are very similar to those of flow units. In fact, the two unit types are not differentiated on the basis of color or morphology, but rather on their location: Patera Flow units occur inside the bounding scarps of the paterae and cover relatively large portions of the interior, whereas Flow units occur outside the scarps of the paterae. Traditionally, Patera Floor and Flow units have been mapped separately (Schaber, 1980, 1982; Crown et al., 1992) because of the ambiguity regarding their compositions and emplacement mechanisms from *Voyager* data. Although analyses of *Galileo* data show that the materials that make up specific colored Patera Floor and Flow units are the same (Geissler et al., 1999; Williams et al., 2002, 2004, 2005), given the spatial resolution of the available data, there is often ambiguity regarding the emplacement mechanism for Patera Floors (i.e., lava lakes vs lava flows).

In the Amirani–Gish Bar region Patera Floor materials range from white–yellow to yellow–orange to greenish to dark black. These colors are inferred to represent specific mixes of compositions, including sulfur–SO_2, various forms of sulfur, alteration products of silicate–sulfur interactions, and relatively fresh silicates, respectively (Williams et al., 2002, 2004; Lopes et al., 2001). The processes that create this variety of Patera Floor materials are complex and not well understood. Hypotheses include the exhumation of sills, tectonic basins filled with lava, and caldera-forming collapses (Keszthelyi et al., 2004; Williams et al., 2002; Radebaugh et al., 2001), and/or partial or complete covering by frozen sulfur and SO_2. Because of the wide color variation in paterae in the Amirani–Gish Bar region, we have defined and characterized only two broad subunits of Patera Floor materials: Bright (pf_b, presumably sulfur- or SO_2-dominated) and Dark (pf_{d1} and pf_{d2}, presumably silicate-dominated). Subunit pf_{d2} is used for the freshest dark flows that occur within paterae, and is equivalent to Flow materials unit f_{d2}.

4.4. Mountain materials

In the Amirani–Gish Bar region we have defined and characterized only one unit for Io's tectonic mountains, which we call Mountain material (m). This unit occurs in six mountains within this region, which appear to be in various states of degradation. The use of one generalized mountain map unit is different from our previous maps (Williams et al., 2002, 2004, 2005), in which we were able to define and characterize up to three mountain units: Lineated, Mottled, and Undivided materials. The reason for this is two-fold: (1) the SSI mosaic used as our basemap for the Amirani–Gish Bar region is of somewhat lower resolution than those used for the previous maps, and (2) the degradation of the I24 images in this basemap further reduces details that might otherwise be discerned. We interpret this unit as tectonically disrupted sections of Io's crust involved in uplift and/or collapse during mountain formation (see Schenk and Bulmer, 1998; McKinnon et al., 2001; Schenk et al., 2001; Turtle et al., 2001; Jaeger et al., 2003 for various models of mountain formation). Topographic information in this area is sparse. The "scrambling" of the low-sun, orbit 124 images of this area renders photoclinometric techniques untenable. The only stereo coverage is regional mapping stereo at 1.4 to 1.6 km/px, with a baseline stereo resolution of approximately 300 m. This resolution is insufficient to identify low plateaus or most geologic units, but in combination with shadow measurements (Schenk et al., 2001) allows us to determine the heights of several of the mountains mapped in this region. These height estimates include: Monan Mons, <5 km; Euxine Mons, 7–7.7 km; Skythia Mons, 5.5 to 6 km; Gish Bar Mons, 10–11 km; and 6 km for the unnamed peak northeast if Estan Patera (Figs. 1b, 4). These structures can be characterized as typical of ionian mountains.

4.5. Diffuse deposits

The more accurate color imaging and higher resolution of the *Galileo* SSI has been invaluable in recognizing the diversity of diffuse deposits on Io's surface. In the Amirani–Gish Bar region we defined and characterized three types of diffuse deposits: bright (yellowish), white, and red. Our interpretation of these colors is related to the (inferred) primary coloring agent. It is important to note that SO_2 is a major (if not dominant) component in all of these deposits (e.g., Douté et al., 2001, 2002, 2004). White Diffuse deposits (d_w) are thought to be generally a sign of purer SO_2. Bright white plumes at the edge of active flow fields have been attributed to the vaporization and refreezing of SO_2 snow by advancing lava flows (Baloga et al., 1982; Kieffer et al., 2000; Milazzo et al., 2001). In general, Bright Diffuse deposits (d_b) have been recognized as rings around some volcanoes, Prometheus being the most prominent example. The interpretation of Bright Diffuse deposits is that they are likely explosive plume deposits colored by yellow sulfur. Red Diffuse deposits (d_r) occur as thin mantles on the plains in our map area. These deposits typically show decreasing optical depth with increasing distance from the vent complex. They have been interpreted as pyroclastic deposits rich in metastable, short-chain sulfur polymers. The metastable S_3 and S_4 allotropes, red when quenched in their high-temperature forms (Spencer et al., 1997), could act as colorizing contaminants within bright, transparent material such as SO_2 (Geissler et al., 1999). The source of this material appears to be primary magmatic S_2 gas (Spencer et al., 2000; Keszthelyi et al., 2001), although Cl-bearing materials have been detected at some vents (Schmitt and Rodriguez, 2003). Spencer et al. (2000) measured the ratio of S and SO_2 gas in the Pele plume and found that there was approximately 7 times more SO_2 than S. This again shows that the coloring agent seen in the SSI images can be a relatively minor component of the surface.

4.6. Structural features and landforms

We have mapped a wide range of structural features in the Amirani–Gish Bar region, including scarps, ridges, grooves, lineaments, and the caldera-like depressions of paterae. Scarps

delineate both mountains and layered plains, and these features contain most of the observed grooves, ridges, and lineaments. There are a few grooves, scarps, and lineaments found in the plains, whereas the flow fields are relatively bereft of these structures.

5. Results

5.1. Stratigraphy and correlation

Although the lack of impact craters renders global correlation of map units by crater statistical methods impossible, regional to local correlations are still possible using superposition relationships and other principles of relative dating. As with the previous regional maps, these correlations tend to be best at sites of active eruptions. For example, in the Amirani–Gish Bar region, variable and ongoing activity at the Amirani–Maui flow field and within Gish Bar Patera can be identified from image comparisons and superposition relations, including older and recent phases of effusive silicate volcanism between *Galileo* flybys (Keszthelyi et al., 2001; Turtle et al., 2004). Mapping overlapping diffuse deposits indicates ongoing venting of at least two volatile gases (SO_2, S_2) from different vents in the Amirani–Maui flow field. However, it is not possible to extract an age relationship between the Amirani flow field and the adjacent (young but not active) Emakong flows to the south. Overall, the stratigraphic picture that arises from our mapping is of extensive continuous and varied volcanic activity. However, it is noteworthy that the currently active lavas are confined within the boundaries of the older flows from the same sources. The current activity appears to be well within the norm for this region: (1) fresh flows superpose plains and older flows, (2) flows extend from patera, (3) flows cover patera floors, (4) some paterae cut mountains.

5.2. Nature of active volcanism

The locations of the most recent effusive eruptions (i.e., the darkest dark flows) correlate with NIMS hot spots, which occur both in Amirani's flow fields and on the floor of Gish Bar Patera and Estan Patera. Hot spots are also associated with the floors of Dusura, Maui, Shango, Monan, Ah Peku, and several unnamed paterae, although there were no visible changes within these paterae. As is common in other areas of Io, diffuse deposits are centered on many of the hot spots. The map area is dominated by the >300-km-long Amirani–Maui flow field. This flow field has existed at least since before the *Voyager* flybys, as its overall areal extent appears unchanged (Fig. 1a). Mapping shows complex stratigraphic relationships between older and younger bright and dark flows in the Amirani flow field, apparently fed by lava tubes and channels. The large areal extent of the N–S component of the Amirani flow field suggests an origin from a long-duration "Flow-dominated" (formerly "Promethean") eruption style (i.e., slowly emplaced, compound flow lobes like inflationary Hawaiian flows), although an early "Explosion-dominated" (formerly "Pillanian") phase with more rapidly emplaced flows cannot be ruled out. While no active bright flows were observed in the *Galileo* data from Amirani, changes in dark flows were observed within Amirani between October 1999 and February 2000 (Keszthelyi et al., 2001). It is now clear that Maui is being fed by Amirani, such that the term "Maui Eruptive Center" as defined in the post-*Voyager* era for the west end of the Amirani–Maui flow field should be revised (this does not apply to the separate Maui Patera, which is also active). Mapping also suggests changes in dark units within parts of the Gish Bar Patera floor, consistent with repeat *Galileo* imaging (Turtle et al., 2004), likely involving lava flows ("Flow-dominated," formerly "Promethean" eruption style) but not necessarily lava lakes ("Intra-Patera," formerly "Lokian" eruption style; Lopes et al., 2004).

5.3. Diffuse deposits and mountains

As stated, both SO_2- and S_2-rich gases are inferred to be venting from within and around the Amirani–Maui flow field, based on the distribution of White and Red Diffuse deposits, respectively. White Diffuse deposits are the most abundant type in the Amirani–Gish Bar region, occurring not only around hot spots but also around bright flows, some cooler patera floors, around fractures and lineaments on and adjacent to mountains, and as isolated patches in the plains. Our mapping provides additional evidence that fractures on Io can serve as vents for the release of SO_2 gas without the release of magma, as noted by Geissler et al. (2004). It is unclear, however, if this is related to volatilization of material above intrusions, or to SO_2-rich fluids migrating along weaknesses in the crust. A large region of Bright Diffuse material occurs in the southwestern part of the map area, the source of which is likely Sobo Fluctus and/or Surya Patera west of the map area. The six mountains and several layered plateaus and mesas that are present in this region show various states of degradation: Euxine Mons, Monan Mons, and the unnamed mountain SW of Maui Patera appear to be relatively flat and degraded, whereas Gish Bar Mons and the unnamed mountain NE of Estan Patera have steep ridges and appear relatively less degraded; Skythia Mons falls between these endmembers. Clearly, the Amirani–Gish Bar region has been an active volcano-tectonic region for some time (since well before the 1979 *Voyager* flybys), as evidenced by the range of degradational states of the mountains, the complex stratigraphy of the flucti, and the large number of active and inactive paterae. Stratigraphically, both explosive and effusive deposits from the active volcanic centers (particularly within Amirani–Maui) are slowly covering older flows, mountains, and plains throughout the region.

5.4. Other key observations

A significant difference between the Amirani–Gish Bar region and the previously mapped regions is recognition that the Amirani and Shango flow fields cover very large areas, and that for Io as a whole, lava flow fields associated with a specific source may have covered far greater areas than the currently active flows from that source. This suggests that the role of flows in resurfacing Io may be under-represented when just looking

at the active flows today. Alternatively, perhaps our previously mapped areas were just different; this issue will be addressed by the global mapping.

The map units within the AEC and around Shango Patera (within the red dashed boundaries in Fig. 4) might be considered "formations," because of the large areal extent of their varied deposits. Also, bright lava flows from Emakong Patera to the south extend into the mapping area. Although no active bright flows were observed, their areal extents around Amirani and Emakong suggest that in some parts of Io, bright (sulfurous?) flows may play an important role in the long-term resurfacing of Io. By extending this mapping to surrounding regions for the global map, it may become clear why there are more bright flows around Amirani and Emakong.

The older parts of the Amirani flow field appear to grade into the surrounding plains. This suggests that the extent and role of lava flows may be yet again larger than we previously thought. It also supports the idea that the plains are composed of interlayered flows and pyroclastic materials, but the visible surface is dominantly a volatile-rich mantle.

Gish Bar and several other paterae have discrete lava flows within their floors, as seen at high resolution in Chaac Patera (Keszthelyi et al., 2001; Williams et al., 2002). This suggests that a significant number of the intra-patera lava units are not lava lakes (cf. Rathbun et al., 2002; Lopes et al., 2004). The floor of the Kilauea caldera may be a good analog to Gish Bar Patera, where rarely the whole floor is covered with an active lake, but normally there are just flows erupted onto the floor (e.g., Carr and Greeley, 1980). Our mapping suggests that caution needs to be applied when equating a hot patera floor with an active lava lake.

Jaeger et al. (2003) noted that the paterae in the Amirani–Gish Bar region are in precisely the locations expected in response to mountains forming via thrust faulting. However, they and Schenk et al. (2001) also noted that many paterae on Io are not associated with any particular mountain. It is curious that the most extensive flow fields like Amirani are not associated with paterae that are themselves associated with mountains. Perhaps this points to the possibility that paterae next to mountains are continually deepened by tectonics, helping to keep the flows confined within their walls. Away from mountains, the lava may have a better chance of overtopping the patera and producing an extensive flow field.

We and others (Jaeger et al., 2003) noted that the long axes of Skythia Mons, Monan Mons, and Gish Bar Mons appear to be subparallel to the N–NE. This is the first time we have seen strong (but circumstantial) evidence for a regional lithospheric stress pattern across part of Io. A key to understanding this is to map the alignments of the long axes of all the mountains (and thus the inferred orientation of possible orogenic thrust faults). This is the type of question we hope to address with the global mapping.

Finally, while they have been seen in other areas on Io, this is the first time that White diffuse deposits have been mapped around a mountain in a regional map. Is this because there are a relatively large number of mountains in this region? Interestingly, the White Diffuse deposits on Monan and Skythia Montes appear to be concentrated on the side of the mountain with the inferred thrust faults (Jaeger et al., 2003). Perhaps a mountain forming by thrusting over a volatile-rich plain would cause pressure melting of the SO_2 and release at the front of the mountain.

5.5. Implications for global geologic mapping

We note a number of key issues for producing a new, post-*Galileo*, global geologic map of Io on the basis of (1) analysis and comparison of our regional map of the Amirani–Gish Bar region to the previous *Galileo*-based regional maps (Williams et al., 2002, 2004, 2005) and to the *Voyager*-era geologic maps (Schaber, 1980, 1982; Moore, 1987; Greeley et al., 1988; Schaber et al., 1989; Whitford-Stark et al., 1991; Crown et al., 1992), (2) study of available data sources for these maps, and (3) examination of the preliminary versions of the new USGS-produced, 1 km/px combined *Galileo–Voyager* global Io mosaics. Because parts of the surface of Io were observed to change within the span of individual *Galileo* flybys (∼1–3 months), a global map alone, completed using the same methods as used for the four regional maps, would be unable to adequately describe the geology of Io. If we map globally at the formation level, and include all of the paterae, flucti, mountains, and visible diffuse deposits, then we will have completed a global reconnaissance of Io and identified the major eruption centers. This in itself is a major advance. However, such a global map will require a higher level of interpretation to define not only the "material" units, but also actual litho-stratigraphic formations, much more akin to true terrestrial geologic maps. This approach was used in the previous global geologic map of Io with good success. Through a comparison of the four *Galileo*-based regional maps (Williams et al., 2002, 2004, 2005; this paper), we find good agreement in our choice of material units and structures, the ability to recognize variation in major feature types, and the capability to correlate volcanic episodes at major eruptive centers. However, it is also clear from the comparison of the regional *Galileo* maps to the *Voyager* global map that the level of detail included on the regional maps can not be represented at the global scale.

The global basemap will necessarily be made up of images that show the surface of Io at a mix of times. To describe the *changes* in some of these features requires more information. A GIS database, where repeat imaging can be assembled in a series of layers seems to be the best solution for recording surface changes and allowing the user to examine data representing the temporal evolution of the surface. This GIS database would have three purposes: (a) to record more detail than can be represented on a printed map sheet where higher resolution images are available; (b) to allow quantitative analyses to be made on the geospatial relationships between different features (e.g., the distributions of hotspots, paterae, volcanic centers, and mountains); and (c) to archive all of the *Galileo* SSI, NIMS, and PPR data alongside *Voyager* data, the global basemaps, and our new geologic map to produce the definitive source of information on Io for future generations of scientists. We envision eventually producing a WWW-accessible database centered on a set

of primary map base layers (i.e., the new global mosaics), with clickable layers to secondary datasets (*Galileo* NIMS and PPR data, *Voyager* data, higher-resolution *Galileo* images and maps, databases of ionian paterae and mountains). The final GIS database could be supplemented with future Earth- and space-based observations of Io as they become available, providing the ultimate data source for Io researchers.

6. Summary

We have constructed a geologic map of the Amirani–Gish Bar region of Io using *Galileo* images, not only to understand better the geology of this region but also to identify (along with reviews of previous *Galileo*- and *Voyager*-based maps) the best methodology to produce a new global geologic map of Io using the recently completed USGS combined *Galileo–Voyager* mosaics. Primary types of material units (plains, patera floors, flows, mountains, and diffuse deposits), first identified from *Voyager* images, continue to serve as a useful foundation for mapping Io using *Galileo* images. All of these units occur in the Amirani–Gish Bar region, which is dominated by the >300-km-long Amirani–Maui flow field (Keszthelyi et al., 2001). Mapping shows that Amirani–Maui is actually a complex flow field composed of bright and dark flows associated with at least 5 hot spots detected by *Galileo*, several of which are active and emplace dark, presumably silicate flows in the "Promethean" eruption style (Keszthelyi et al., 2001). The so-called "Maui Eruptive Center" is actually a flow fed by Amirani, and use of this term should be revised. Both SO_2- and S_2-rich gases are venting from various sources both at Amirani and throughout the region, including hot spots, paterae, flow margins, and fractures in the mountains and plains not otherwise associated with volcanism. At least six tectonic mountains (and no volcanic edifices) occur in this region, and they are in various states of degradation, attesting to the long volcano-tectonic history of this region.

The implications from our mapping of this region, in conjunction with analysis of previous mapping, suggests to us that a new global geologic map of Io will require not only a USGS map sheet displaying the global types and distribution of key volcanic units (paterae, flucti, hot spots, plume sources), mountains, and other features, but also must include a means of recording surface changes due to Io's active volcanism (e.g., measuring the areal extents and distributions of active flow fields and explosively emplaced diffuse deposits that fade with time). This will be done through a GIS database, which will contain the new mosaics, our maps, and all available *Galileo* and *Voyager* data at global to regional resolutions. This database is necessary to synthesize knowledge of Io's surface geology at a global scale, which is fundamental for the full interpretation of observations acquired by the *Galileo* PPR and NIMS instruments at lower spatial resolutions than SSI images. This approach is particularly useful for the *Galileo* data, because there is temporal coverage over many parts of Io that enables the determination of waxing and waning volcanism at particular hot spots. Finally, a global map produced in this way will serve as a framework for the continuing analysis of *Galileo* data, will be a useful tool for correlating ongoing ground-based telescopic observations of Io with known sites of active volcanism, and will be a key element in planning spacecraft observations of Io from any future missions.

Acknowledgments

The authors thank Louise Prockter and an anonymous reviewer for helpful comments. This work was funded under NASA Outer Planets Research Program Grant Number NNG05GH43G to David A. Williams.

References

Baloga, S.M., Pieri, D.C., Matson, D.L., 1982. Regolith outgassing by sulfur flows on Io. NASA Tech. Mem. 85127, 5–7.

Bart, G.D., Turtle, E.P., Jaeger, W.L., Keszthelyi, L.P., Greenberg, R., 2004. Ridges and tidal stress on Io. Icarus 169, 111–126.

Carlson, R.W., Smythe, W.D., Lopes-Gautier, R.M.C., Davies, A.G., Camp, L.W., Mosher, J.A., Soderblom, L.A., Leader, F.E., Mehlman, R., Clark, R.N., Fanale, F.P., 1997. The distribution of sulfur dioxide and other infrared absorbers on the surface of Io. Geophys. Res. Lett. 24, 2479–2482.

Carr, M.H., 1986. Silicate volcanism on Io. J. Geophys. Res. 91, 3521–3532.

Carr, M.H., Greeley, R., 1980. Volcanic Features of Hawaii: A Basis for Comparison with Mars. NASA SP-403. NASA, Washington, DC.

Crown, D.A., Greeley, R., Craddock, R.A., Schaber, G.G., 1992. Geologic map of Io. U.S. Geol. Surv. Misc. Invest. Series Map I-2209, 1:15,000,000, Reston, VA.

Davies, A.G., Keszthelyi, L.P., Williams, D.A., Phillips, C.B., McEwen, A.S., Lopes-Gautier, R.M., Smythe, W.D., Soderblom, L.A., Carlson, R.W., 2001. Thermal signature, eruption style, and eruption evolution at Pele and Pillan on Io. J. Geophys. Res. 106, 33079–33103.

Douté, S., Schmitt, B., Lopes-Gautier, R., Carlson, R., Soderblom, L., Shirley, J., and the Galileo NIMS Team, 2001. Mapping SO_2 frost on Io by the modeling of NIMS hyperspectral images. Icarus 149, 107–132.

Douté, S., Lopes, R., Kamp, L.W., Carlson, R., Schmidt, B., and the Galileo NIMS Team, 2002. Dynamics and evolution of SO_2 gas condensation around Prometheus-like volcanic plumes on Io as seen by the Near Infrared Mapping Spectrometer. Icarus 158, 460–482.

Douté, S., Lopes, R., Kamp, L.W., Carlson, R., Schmidt, B., and the Galileo NIMS Team, 2004. Geology and activity around volcanoes on Io from the analysis of NIMS spectral images. Icarus 169, 175–196.

Geissler, P.E., McEwen, A.S., Keszthelyi, L., Lopes-Gautier, R., Granahan, J., Simonelli, D.P., 1999. Global color variations on Io. Icarus 140, 265–282.

Geissler, P., McEwen, A., Phillips, C., Simonelli, D., Lopes, R.M.C., Douté, S., 2001. Galileo imaging of SO_2 frosts on Io. J. Geophys. Res. 106, 33253–33266.

Geissler, P., McEwen, A., Phillips, C., Keszthelyi, L., Spencer, J., 2004. Surface changes on Io during the Galileo mission. Icarus 169, 29–64.

Greeley, R., Spudis, P.D., Guest, J.E., 1988. Geologic map of the Ra Patera area of Io. U.S. Geol. Surv. Misc. Invest. Series Map I-1949, 1:2,000,000, Reston, VA.

Hapke, B., 1989. The surface of Io: A new model. Icarus 79, 56–74.

Jaeger, W.L., Turtle, E.P., Keszthelyi, L.P., Radebaugh, J., McEwen, A.S., Pappalardo, R.T., 2003. Orogenic tectonism on Io. J. Geophys. Res. 108 (E8), doi:10.1029/2002JE001946. 5093.

Johnson, T.V., Veeder, G.J., Matson, D.L., Brown, R.H., Nelson, R.M., Morrison, D., 1988. Io: Evidence for silicate volcanism in 1986. Science 242, 1280–1283.

Keszthelyi, L.P., McEwen, A.S., Phillips, C.B., Milazzo, M., Geissler, P.E., Williams, D.A., Turtle, E., Radebaugh, J., Simonelli, D., and the Galileo SSI Team, 2001. Imaging of volcanic activity on Jupiter's moon Io by Galileo during GEM and GMM. J. Geophys. Res. 106, 33025–33052.

Keszthelyi, L., Jaeger, W.L., Turtle, E.P., Milazzo, M., Radebaugh, J., 2004. A post-Galileo view of Io's interior. Icarus 169, 271–286.

Kieffer, S.W., Lopes-Gautier, R., McEwen, A., Smythe, W., Keszthelyi, L., Carlson, R., 2000. Prometheus: Io's wandering plume. Science 288, 1204–1208.

Lopes-Gautier, R., and 13 colleagues, 1999. Active volcanism on Io: Global distribution and variations in activity. Icarus 140, 243–264.

Lopes, R.M.C., and 14 colleagues, 2001. Io in the near infrared: NIMS results from the Galileo fly-bys in 1999 and 2000. J. Geophys. Res. 106, 33053–33078.

Lopes, R.M.C., and 13 colleagues, 2004. Lava lakes on Io? Observations of Io's volcanic activity from Galileo NIMS during the 2001 fly-bys. Icarus 169, 140–174.

McEwen, A.S., and 13 colleagues, 1998a. Active volcanism on Io as seen by Galileo SSI. Icarus 135, 181–219.

McEwen, A.S., and 14 colleagues, 1998b. High-temperature silicate volcanism on Jupiter's moon Io. Science 281, 87–90.

McEwen, A.S., Lopes-Gautier, R., Keszthelyi, L., Kieffer, S.W., 2000a. Extreme volcanism on Jupiter's moon Io. In: Zimbelman, J.R., Gregg, T.K.P. (Eds.), Environmental Effects on Volcanic Eruptions: From Deep Oceans to Deep Space. Kluwer Academic/Plenum Publishers, New York, pp. 179–205.

McEwen, A.S., and 25 colleagues, 2000b. Galileo at Io: Results from high-resolution imaging. Science 288, 1193–1198.

McKinnon, W.B., Schenk, P.M., Dombard, A.J., 2001. Chaos on Io: A model for formation of mountain blocks by crustal heating, melting, and tilting. Geology 29, 103–106.

Milazzo, M.P., Keszthelyi, L.P., McEwen, A.S., 2001. Observations and initial modeling of lava–SO_2 interactions at Prometheus, Io. J. Geophys. Res. 106, 33121–33128.

Moore, H.J., 1987. Geologic map of the Maasaw Patera area of Io. U.S. Geol. Surv. Misc. Invest. Series Map I-1851, 1:1,003,000, Reston, VA.

Moore, J.M., Sullivan, R.J., Chuang, F.C., Head III, J.W., McEwen, A.S., Milazzo, M.P., Nixon, B.E., Pappalardo, R.T., Schenk, P.M., Turtle, E.P., 2001. Landform degradation and slope processes on Io: The Galileo view. J. Geophys. Res. 106, 33223–33240.

Peale, S.J., Cassen, P., Reynolds, R.T., 1979. Melting of Io by tidal dissipation. Science 203, 892–894.

Radebaugh, J., Keszthelyi, L.P., McEwen, A.S., Turtle, E.P., Jaeger, W., Milazzo, M., 2001. Paterae on Io: A new type of volcanic caldera? J. Geophys. Res. 106, 33005–33020.

Radebaugh, J., McEwen, A.S., Milazzo, M.P., Keszthelyi, L.P., Davies, A.G., Turtle, E.P., Dawson, D.D., 2004. Observations and temperatures of Io's Pele Patera from Cassini and Galileo spacecraft images. Icarus 169, 65–79.

Rathbun, J.A., Spencer, J.R., Davies, A.G., Howell, R.R., Wilson, L., 2002. Loki, Io: A periodic volcano. Geophys. Res. Lett. 29 (10), doi:10.1029/2002GL014747.

Sagan, C., 1979. Sulfur flows on Io. Nature 280, 750–753.

Schaber, G.G., 1980. The surface of Io: Geologic units, morphology and tectonics. Icarus 43, 302–333.

Schaber, G.G., 1982. The geology of Io. In: Morrison, D. (Ed.), Satellites of Jupiter. Univ. of Arizona Press, Tucson, pp. 556–597.

Schaber, G.G., Scott, D.H., Greeley, R., 1989. Geologic map of the Ruwa Patera quadrangle (Ji-2) of Io. U.S. Geol. Surv. Geol. Invest. Series Map I-1980, 1:5,000,000, Reston, VA.

Schenk, P.M., Bulmer, M.H., 1998. Origin of mountains on Io by thrust faulting and large-scale mass movements. Science 279, 1514–1517.

Schenk, P., Hargitai, H., Wilson, R., McEwen, A., Thomas, P., 2001. The mountains of Io: Global and geological perspectives from Voyager and Galileo. J. Geophys. Res. 106, 33201–33222.

Schmitt, B., Rodriguez, S., 2003. Possible identification of local deposits of Cl_2SO_2 on Io from NIMS/Galileo spectra. J. Geophys. Res. 108 (E9), doi:10.1029/2002JE001988. 5104.

Shoemaker, E.M., Hackman, R.J., 1962. Stratigraphic basis for a lunar time scale. In: Kopal, Z., Mikhailov, Z.K. (Eds.), The Moon. Academic Press, London, pp. 289–300.

Spencer, J.R., Sartoretti, P., Ballester, G.E., McEwen, A.S., Clarke, J.T., McGrath, M., 1997. The Pele plume (Io): Observations with the Hubble Space Telescope. Geophys. Res. Lett. 24, 2471–2474.

Spencer, J.R., Jessup, K.L., McGrath, M.A., Ballester, G.E., Yelle, R., 2000. Discovery of gaseous S_2 in Io's Pele plume. Science 288, 1208–1210.

Tanaka, K.L., and 11 colleagues, 1994. The Venus Geologic Mappers Handbook. USGS Open-File Rep. 94-438, 66 pp.

Turtle, E.P., and 10 colleagues, 2001. Mountains on Io: High-resolution Galileo observations, initial interpretations, and formation models. J. Geophys. Res. 106, 33175–33200.

Turtle, E.P., and 14 colleagues, 2004. The final Galileo SSI observations of Io: Orbits G28–I33. Icarus 169, 3–28.

Whitford-Stark, J.L., Mouginis-Mark, P.J., Head, J.W., 1991. Geologic map of the Lerna region (Ji-4) of Io. U.S. Geol. Surv. Misc. Invest. Series Map I-2055, 1:5,000,000, Reston, VA.

Wilhelms, D.E., 1972. Geologic Mapping of the Second Planet. USGS Inter-Agency Rep., Astrogeology 55.

Wilhelms, D.E., 1990. Geologic mapping. In: Greeley, R., Batson, R.M. (Eds.), Planetary Mapping. Cambridge Univ. Press, Cambridge, UK, pp. 208–260.

Williams, D.A., Wilson, A.H., Greeley, R., 2000. A komatiite analog to potential ultramafic materials on Io. J. Geophys. Res. 105, 1671–1684.

Williams, D.A., Greeley, R., Lopes, R.M.C., Davies, A.G., 2001. Evaluation of sulfur flow emplacement on Io from Galileo data and numerical modeling. J. Geophys. Res. 106, 33161–33174.

Williams, D.A., Radebaugh, J., Keszthelyi, L.P., McEwen, A.S., Lopes, R.M.C., Douté, S., Greeley, R., 2002. Geologic mapping of the Chaac–Camaxtli region of Io from Galileo imaging data. J. Geophys. Res. 107, doi:10.1029/2001JE001821. 5068.

Williams, D.A., Schenk, P.M., Moore, J.M., Keszthelyi, L.P., Turtle, E.P., Jaeger, W.L., Radebaugh, J., Milazzo, M.P., Lopes, R.M.C., Greeley, R., 2004. Mapping of the Culann–Tohil region of Io from Galileo imaging data. Icarus 169, 80–97.

Williams, D.A., Keszthelyi, L.P., Schenk, P.M., Milazzo, M.P., Lopes, R.M.C., Rathbun, J.A., Greeley, R., 2005. The Zamama–Thor region of Io: Insights from a synthesis of mapping, topography, and Galileo spacecraft data. Icarus 177, 69–88.

Young, A.T., 1984. No sulfur flows on Io. Icarus 58, 197–226.